Adıyaman University
Journal of Engineering Sciences
Adyü J Eng Sci 2025;12(26):211-224
Adıyaman Üniversitesi
Mühendislik Bilimleri Dergisi
Adyü Müh Bil Derg 2025;12(26):211-224
https://doi.org/10.54365/adyumbd.1696358

Research Article / Araştırma Makalesi

Investigation of Response of Embedded Pipe in Two-Layered Soil Subjected to Near-Fault and Far-Fault Earthquakes

Yakın Fay ve Uzak Fay Depremlerine Maruz Kalan İki Katmanlı Zemindeki Gömülü Borunun Tepkisinin Araştırılması

Kaşif Furkan Öztürk [1*]

[1] Gümüşhane University, Faculty of Engineering and Natural Sciences, Department of Civil Engineering, Gümüşhane/ Türkiye

Abstract

The behavior of pipelines during earthquakes depends on many factors such as fault movements, soil types, pipe material properties and connection details. On the other hand, damages in pipeline systems can also be seen due to relatively high peak ground acceleration values caused by wave propagation effects, or liquefaction, surface rupture that may be triggered by earthquakes. In this context, in the scope of the study, the effects of soil-structure interaction phenomenon as well as near-fault and far-fault earthquake effects on the behaviors of the pipe system have been investigated using the developed two-dimensional finite element model. Modal analyses of soil-pipe interaction system have been made for the different soil conditions and dominant mode frequencies of interaction system have been compared with dominant site frequencies obtained using a well-known approach. In addition, parametric analyses have been performed in the time domain using different soil systems and earthquake loadings. The changes in the behaviors of the pipe system have been comparatively examined for different soil conditions and earthquake loadings considered. The obtained results importantly draw attention to the fact that the responses of the pipe system may vary depending on the soil-pipe interaction, near-fault and far-fault earthquake loadings.

Keywords: *ANSYS, Finite element analysis, Pipeline, Near-fault earthquake, Soil-pipe interaction*

Öz

Boru hatlarının deprem sırasındaki davranışı, fay hareketleri, zemin tipleri, boru malzemesinin özellikleri ve bağlantı detayları gibi birçok faktöre bağlıdır. Diğer yandan, depremler tarafından tetiklenebilen sıvılaşma, yüzey kırığı veya dalga yayılım etkilerinin neden olduğu nispeten yüksek tepe yer hareketi ivme değerlerinden dolayı da boru hattı sistemlerinde hasarlar görülebilir. Bu bağlamda, çalışma kapsamında, geliştirilen iki boyutlu sonlu elemanlar modeli kullanılarak, zemin-yapı etkileşim olgusunun yanı sıra yakın fay ve uzak fay deprem etkilerinin boru sisteminin davranışları üzerindeki etkileri araştırılmıştır. Zemin-boru etkileşim sisteminin modal analizleri, farklı zemin koşulları için yapılmış ve etkileşim sisteminin temel mod frekansları, iyi bilinen bir yaklaşım kullanılarak elde edilen saha temel frekansları ile karşılaştırılmıştır. Ayrıca, farklı zemin sistemleri ve deprem yüklemeleri kullanılarak zaman alanında parametrik analizler gerçekleştirilmiştir. Boru sisteminin davranışlarındaki değişimler, dikkate alınan farklı zemin koşulları ve deprem yüklemeleri için karşılaştırmalı olarak incelenmiştir. Elde edilen sonuçlar, boru sisteminin tepkilerinin zemin-boru etkileşimine, yakın fay ve uzak fay deprem yüklerine bağlı olarak değişebileceğine önemli ölçüde dikkat çekmektedir.

Anahtar Kelimeler: *ANSYS, Sonlu Eleman Analizi, Boru Hattı, Yakın Fay Depremi, Zemin-boru Etkileşimi*

[*] Corresponding e-mail (Sorumlu yazar e-posta): kasiffurkan.ozturk@gumushane.edu.tr
Received (Geliş Tarihi):09.05.2025, **Accepted (Kabul Tarihi):** 09.07.2025

1. Introduction

Pipelines are frequently used in the transportation of various gases and liquids due to their advantages such as relatively low operating costs, continuity, environmental friendliness and efficiency over long distances compared to other transportation methods as an important element of infrastructure systems. The prevalence of pipeline systems, especially in natural gas transportation and the increasing use of these structural systems draw attention to the importance of pipeline systems in terms of continuous serviceability.

Damages that may occur in pipeline systems may develop due to many effects. Some of the best-known possible causes are liquefaction, lateral spreading, exposure to high ground acceleration, slope failure, and surface collapse [1]. In addition to these causes, many researchers have investigated the behavior of pipelines under fault movement with parametric studies. Vazouras et al. [2] parametrically investigated the behavior of different steel pipes for different fault movement displacements under a strike-slip fault. The researchers emphasized that loose sand conditions in cohesionless soils caused larger critical failure displacements than dense soil conditions. Xu et al. [3] emphasized that there were two possible local buckling damage, located on the hanging and foot wall block sides of the buried pipeline system under oblique-reverse fault movement, respectively. Saiyar et al. [4] conducted four centrifuge experiments to investigate the behavior of flexible pipelines under normal fault motion, showing that the curvature distributions along the model pipes are not strictly anti-symmetric with respect to the soil shear line and show larger absolute peaks in the bearing region. Additionally, the researchers found that pipe curvatures are a function of the pipe's bending stiffness (E_pI_p), and higher pipe stiffness leads to consistently lower curvature values, as expected. Wang et al. [5] has developed an intelligent framework to predict the reliability evolution of natural gas pipelines under earthquake effects. As a method, a new hybrid machine learning model is constructed using a Backpropagation Neural Network model integrated with the Lévy Flight Strategy and the Sparrow's Search Algorithm. Model proposed by researchers improves the prediction accuracy and is effective in identifying the impact of parameter uncertainties. Pan et al. [6] has investigated the seismic performance of free-span submarine pipelines under offshore spatial earthquake motions using underwater shaking table tests and numerical simulations. Researchers have showed that the earthquake excitation type, coherence loss effect and ground motion directionality significantly affect the seismic behavior of pipelines. Darvishi et al. [7] has developed performance-based curves using numerical simulations for the fragility analysis of buried pipelines subjected to earthquake-induced landslides in Iran. The results showed that increasing the pipe diameter and stiffening the landslide boundary interface significantly improved the earthquake performance by reducing pipe deformation. Toprak et al. [8] has examined the effects of the February 6, 2023 Kahramanmaraş earthquake on water transmission and distribution systems through detailed field observations and institutional interviews. The findings revealed the damages in water systems after the earthquake, repair processes, and the importance of disaster-resistant infrastructure design and communication between institutions. Uckan et al. [9] has conducted field observations and analyses to investigate the damage status of underground natural gas and water pipelines in the February 6, 2023 Kahramanmaraş earthquake. As a result, researchers have determined that pipelines, especially in fault transition areas, suffered major deformations and flexible connections have important in these regions.

Static and dynamic analyses of soil-pipe interaction systems can be performed using many approaches. Dynamic analyses of these systems can be grouped under three main headings such as analysis the longitudinal direction, plane strain and plane stress analysis. The well-known analytical approach used in longitudinal dynamic analyses of the pipeline is the lumped mass approach. In this approach, the mass-spring-damper system is created and the pipeline system is solved by creating the motion equation [10]. In addition, the effect of spatial change between different freedom points along the pipeline can be included in the solution with the cross terms in the stiffness and damping matrices of the soil system [11]. Another approach frequently preferred for the static [12] or the dynamic analysis [13] of pipelines is the modeling of the pipeline along its length using the shell and beam element types (hybrid approach) by the

help of the finite element/finite difference method. In this approach, the pipe-soil interaction system can be created by representing the soil environment with the help of spring or solid elements after selecting a length that will not be affected by the boundary effects of the pipe system. In addition, while considering soil-pipeline interaction system, the behavior of soil medium around pipeline system can be imitated spring or solid elements. This approach adopted to model the soil-pipe interaction system is frequently used in the investigation of the seismic behavior of natural gas pipelines modeled using beam elements and passing through the ocean floor [13,14]. On the other hand, the effect of earthquake motion can affect especially long structural systems with some time delay. This effect can cause significant changes in the behavior of such structural systems compared to the assumption of simultaneous effects [15]. In this context, it is an important issue to consider the effect of time delay due to spatial change expressed in the dynamic analyses of long structural systems such as pipelines and tunnel structures [16] and this effect should be included in dynamic analyses. When investigating the dynamic behavior of pipe-soil interaction systems, the plane strain or plane stress analysis can be performed using the cross-section of the pipe system. Model in the plane strain analyses is consisted of soil and pipe system where are modeled with two-dimensional (2D) solid elements. On the other hand, performing in the plane stress analyses, while the pipe system is modeled by 2D solid elements, the rigidity and radiational damping of the soil system are modeled with the help of spring elements [15]. Datta [15] has shown that the models used in these two analysis methods can significantly overlap for the displacements obtained from the dynamic analyses.

In this study, the soil-pipe interaction system has been developed as 2D using the ANSYS package program [17] and the plane strain analyses of developed model have been carried out depending on the time. In the parametric analyses, the dynamic responses of the pipe system have been examined for four different soil systems and six different ground motions by considering the internal pipe pressure. The research findings have been presented in terms of pipe displacements and von Mises stress responses for different soil systems as well as earthquakes. The results draw attention to the fact that the soil-pipe interaction system and near-far-fault earthquakes can significantly change the pipe responses.

2. Finite element model developed for the soil-pipe interaction system

While considering the soil-pipe interaction problem, plane strain conditions have been taken into account in the finite element model due to the fact that the in-plane lengths of the pipe and soil medium are quite long. While modeling the soil and pipe systems, the four-node PLANE182 element type with two degrees of freedom at each node have been used. This element type is frequently preferred by many researchers [18–20] in linear and nonlinear earthquake analyses due to plasticity, hyperelasticity, stress stiffening, large deflection, and large strain capabilities. Additionally, in most cases, the element can be used with four nodes, which makes it particularly easy to define viscous boundaries. In this context, while modeling the soil, it is truncated as a semi-infinite environment by considering the calculation time and solution costs. In this modeling approach, while selecting the soil boundaries, the damping approach proposed by Lysmer and Kuhlemeyer [21] have been adopted at the model side boundaries in order to prevent the effects of the waves reflecting from the boundaries. For this objective, the MATRIX27 element type has been used on the side faces of the model for the damping. The soil system has been considered as 30 m from the ground surface to the bedrock and it has been assumed that there is a bedrock at the base of the soil system. In addition, the lower boundary of the soil medium and the tip of the viscous elements are fixed support. The proposed finite element model is shown in Figure 1.

While creating the mesh structure, a denser mesh structure has been especially preferred in the region around the pipe, and a coarser mesh has been used in regions far from the pipe system to provide a balance between analysis time and accuracy. In addition, mesh sensitivity analysis has been performed to evaluate the effect of mesh density on the fundamental frequencies of the soil-pipe interaction system and appropriate mesh density has been selected in the finite element model. Use of coarse meshes can lead to filtering of high-frequency components. Therefore, the element dimensions in the finite element model should be limited with $h_{max} \leq (V_s / (N * f_{max}))$ [22], where h_{max}, f_{max} and N define maximum element

dimension, the highest frequency of earthquake, typically a number between 5 and 8 [22]. In this context, h_{max} has been selected as 0.50 m for N=7 [23] and f_{max}=25 Hz [22], taking into account the shear wave velocities in different soil layers. On the other hands, the minimum element dimensions for the soil and pipe systems have been considered as 47.865 mm and 9.550 mm, respectively.

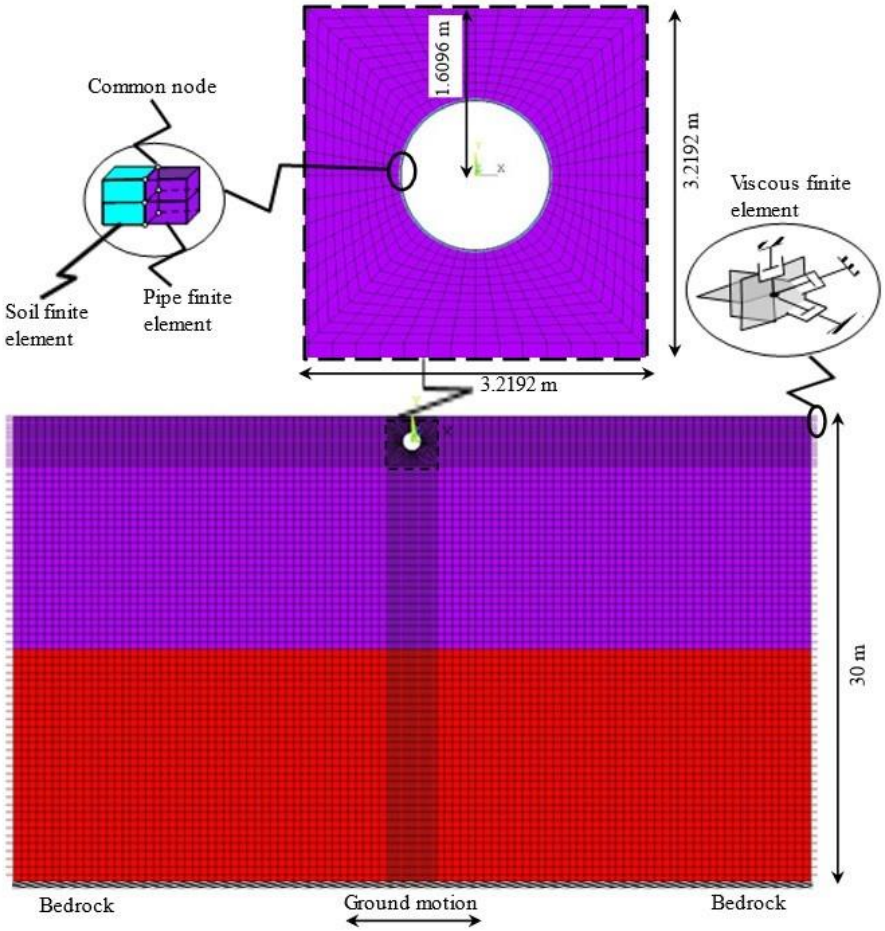

Figure 1. Finite element model proposed for the soil-pipe interaction system

The pipe system is X65 type steel and the burial depth is 1.6096 m from the pipe center to the surface. The outer diameter, wall thickness, density, Poisson's ratio, elasticity modulus and yield stress values of the pipe system are considered as 1.2192 m, 0.0191 m, 7850 kg/m3, 0.3, 210 GPa and 448 MPa, respectively. Based on the assumption that no significant contact will be lost between the soil and the pipe system, the soil-pipe interface is modeled with the common node approach. This approach is frequently used when investigating the dynamic behavior of structures [24–26]. Under such an assumption, when solving the soil-pipe interaction problem, the mass, stiffness and damping expressions resulting from common nodes in the force equilibrium of the system consist of the sum of the contributions obtained from soil and pipe systems.

3. Parametric analyses performed in time domain

The properties of the soil systems considered for the purpose of investigating the effects of the soil-pipe interaction system are shown in Table 1. In this context, the parametric analyses of the soil-pipe interaction system have been carried out in two stages within the scope of the study. In the first stage, before moving on to the time history analyses, the mode selections of the soil-pipe interaction system have been obtained with the help of Block Lanczos type modal analyses. In the ANSYS package program, the solution of the eigenvalue problem can be achieved with the help of different techniques. However, Block Lanczos approach can provide relatively fast solutions for obtaining the modes of systems with a high number of degrees of freedom or extracting high mode numbers. For these reasons, Block Lanczos analyses for

different soil-pipe interaction systems have been performed to select the fundamental modes in the x direction, which is the direction of the seismic excitation. As a result of the modal analyses, it has been seen that the effective masses and mode shapes of the interaction systems have been examined and the dominant frequencies have been obtained in the 1st and 3rd modes. After this, the Rayleigh damping coefficients have been calculated. Damping ratios of soil and pipe system have been taken into account as 0.02 and 0.05, respectively. In addition, in the analyses carried out in the time domain, the internal pipe pressure has been considered as 8 MPa and the bilinear isotropic hardening material model for the nonlinear behavior of the pipe system has been used. Moreover, the behavior of the soil system has been assumed to be linear elastic, as this assumption allows to consider the basic soil properties in a practical way. Soil properties adopted for the parametric studies in Table 1 have been selected based on literature [27,28].

Table 1. Soil properties used in the study

ID	Location of layer	Soil profile	E, MPa	v (-)	p, kN/m^3	V_s, m/s
S1-S1	Upper layer	S1	300.0	0.30	2100	234.4
	Lower layer	S1	300.0	0.30	2100	234.4
S1-S2	Upper layer	S1	300.0	0.30	2100	234.4
	Lower layer	S2	150.0	0.30	1900	174.3
S1-S3	Upper layer	S1	300.0	0.30	2100	234.4
	Lower layer	S3	75.0	0.30	1800	126.6
S1-S4	Upper layer	S1	300.0	0.30	2100	234.4
	Lower layer	S4	37.5	0.30	1700	92.1

E: Young's modulus, v: Poisson ratio, p: Density, V_s: Shear wave velocity

The earthquake excitations considered in full-transient analyses are grouped into two as near-fault and far-fault. When the earthquakes are recorded in fields located 10 km or more away from the fault rupture, it is generally stated as far-fault earthquake [29–31]. This distance have been accepted arbitrarily in the near-fault and far-fault earthquake definitions [30] and is not mandatory depending on many other factors [32]. Fault rupture distance have been defined as 15 km [33,34] [19] or 20 km [35,36] in many researches. On the other hand, the near-fault ground motions is recorded at locations closer than 10 km to the fault rupture [30]. In addition, the near-fault ground motions generally have a velocity pulse period (T_p) which is greater than 1 s and the ratio of peak ground velocity (PGV) to peak ground acceleration (PGA) is greater than 0.1 s [37]. In this context, the earthquakes considered for analyses have been obtained from the Pacific Earthquake Engineering Research (PEER) Next Generation Attenuation phase 2 [38] database by taking into account the stated criteria. The characteristics of the earthquakes used are shown in Table 2.

Table 2. Earthquakes used in parametric analyses

ID	RSN	Ground Motion	Earthquake name	M_w	Component	Rrup (km)	V_{s30}	PGV (m/s)	PGA (m/s^2)	PGV/PGA (s)	Rjb (km)	T_p (s)
NF-1	1045	NF	Northridge-01	6.69	046	5.48	285.93	1.18	4.11	0.29	2.11	3.00
FF-1	988	FF	Northridge-01	6.69	360	23.41	277.98	0.25	2.17	0.12	15.53	-
NF-2	1054	NF	Northridge-01	6.69	L	7.46	325.67	0.76	5.47	0.14	5.54	1.23
FF-2	1039	FF	Northridge-01	6.69	180	24.76	341.58	0.20	2.86	0.07	16.92	-
NF-3	1120	NF	Kobe	6.90	000	1.47	256.00	1.21	6.06	0.20	1.46	1.86
FF-3	1105	FF	Kobe	6.90	000	95.72	256.00	0.15	1.37	0.11	95.72	-

NF: Near-fault earthquake with velocity pulse; FF: Far-fault earthquake, RSN: Record sequence number of earthquakes obtained from PEER ground motion database, Rrup: Closest distance from site to the rupture surface, Rjb: Closest horizontal distance from site to the rupture plane

4. Result and discussion

The pipe-soil system is examined within the framework of three basic concepts. The first of these is comparisons made between the simplified site frequencies and the dominant frequencies of the finite element model developed for soil-structure interaction system using soil-pipe bending stiffness ratio. Second and third of these have focused on to discuss the soil-structure interaction effect and the earthquake effects depending on the near and far-fault, respectively. In this context, the findings obtained from the parametric analyses are examined in detail under the following subheadings.

4.1. Dominant mode frequencies of the soil-pipe interaction system

The soil-structure interaction system can affect the behavior of buried pipe systems. In order to understand this effect mechanism, the stiffness ratio between the soil and the pipe system is an important parameter. In other words, these stiffness ratios can be significantly related to both the dominant mode frequencies of the interaction system and the dynamic behavior of the pipe system. For these reasons, the soil-pipe bending stiffness ratio can be written as follows, depending on the mutual interaction of the soil and the pipe system [39]:

$$S_p = \frac{M_s R^3}{E_p I_p} \tag{1}$$

In this equation, M_s, E_p, I_p and R define the constrained modulus of the soil, the elasticity modulus of the pipe, the moment of inertia of the pipe and the distance from the center of the pipe wall to the center of the pipe (the radius), respectively. Here, M_s and I_p can be expressed as follows, respectively:

$$M_s = \frac{E(1-v)}{(1+v)(1-2v)} \tag{2}$$

$$I_p = \frac{t^3}{12} \tag{3}$$

In the above equation, t defines the wall thickness of the pipe system.

It is particularly useful to emphasize here that E and v for the constrained modulus defined in Equation 2 can be taken as weighted average values (e.g. E_{av}, v_{av}) since the soil profiles considered in the study have been consisted of two layers. In this context, the weighted average elasticity modulus (E_{av}) and Poisson's ratio (v_{av}) values for the soil systems are found as following:

$$E_{av} = \frac{E_U * H_U + E_L * H_L}{H_U + H_L} \tag{4}$$

$$v_{av} = \frac{v_U * H_U + v_L * H_L}{H_U + H_L} \tag{5}$$

Where E_U, E_L, H_U, H_L, v_U and v_L are Young's modulus of upper and lower layer, thickness of upper layer, thickness of lower layer, Poisson's ratio of upper layer and Poisson's ratio of lower layer, respectively. Depending on soil layers, the values of E_{av} and v_{av} are shown in Table 3.

Table 3. Weighted average values of E_{av} and v_{av} based on soil layers

ID	E_{av}, MPa	v_{av} (-)
S1-S1	300.0	0.30
S1-S2	225.0	0.30
S1-S3	187.5	0.30
S1-S4	168.8	0.30

When investigating the dynamic behavior of the soil-pipe interaction system, it is important issue to find the dominant mode frequencies of the interaction system by performing modal analysis. In partially or completely buried structural systems, the behavior of the structural system can be significantly governed by the soil medium depending on the interaction between the structure and the soil system. In this context, the site frequencies can be important to understand the dynamic response of the pipe system and can be obtained as expressed below [40]:

$$T_{Sp} = \sum_{i=1}^{N-1} \frac{4H_i}{V_i};\ S_f = \frac{1}{T_{Sp}} \tag{6}$$

Where T_{Sp}, S_f, N, V_i and H_i, and define the site period, the site frequency, the number of the layer boundary, the shear velocity and thickness of ith layer.

Stiffness ratios, the site frequencies and the dominant frequencies of the soil-pipe interaction system has been shown in Table 4. Stiffness ratios have been obtained as 715.55, 536.66, 447.22 and 402.50 for the S1-S1, the S1-S2, the S1-S3 and the S1-S4, respectively. It is worth emphasizing that stiffness ratio decreases as expected, considering that the pipe properties are kept constant and the soil stiffness decreases from S1-S1 to S1-S4. Furthermore, when Table 4 is examined, it is clearly understood that the dominant frequencies of the soil-pipe interaction system decrease from S1-S1 to S1-S4 due to the decrease in the stiffness ratio of the soil-pipe interaction system. A similar trend is observed in the dominant frequencies of the soil systems and the dominant frequency of the site system have decreased from S1-S1 to S1-S4.

Table 4. Dominant frequencies obtained from finite element model and site

Soil profile	S_p (-)	Mode direction	Mode characters	SPI_f	S_f
S1-S1	715.55	x	Mode no.	1	1
			Mode frequency (Hz)	1.62	1.95
			RET (%)	71	---
S1-S2	536.66	x	Mode no.	1	1
			Mode frequency (Hz)	1.21	1.67
			RET (%)	74	---
S1-S3	447.22	x	Mode no.	1	1
			Mode frequency (Hz)	0.88	1.37
			ETO (%)	76	---
S1-S4	402.50	x	Mode no.	1	1
			Mode frequency (Hz)	0.64	1.10
			RET (%)	77	---

RET: Ratio of the effective mass to total mass, SPI_f: Dominant frequency of soil-pipe interaction system

Depending on the problem at hand, while selecting the dominant mode frequencies of the interaction system, the effective mode masses and mode shapes of the system can be used. On the other hand, in order to understand the relationship between the dominant mode frequencies of the interaction system and the

site system, it is important to make a comparison between the frequencies. For example, when Table 4 is analyzed, while the dominant frequency of the site is 1.95 Hz for the S1-S1 soil system, it is understood that the same frequency value is 1.62 Hz for the soil-pipe interaction system. As can be clearly seen from the example, the dominant frequency value obtained for the soil-pipe interaction system is obtained with a decrease by 16.9% compared to the dominant site frequency. In addition, the dominant frequency emphasized for soil-pipe interaction system here may be considered as the frequency of the coupled sway mode of the soil-pipe interaction system, when Figure 2a and Table 4 are examined. Similar change trends between frequencies can also be easily seen for the S1-S2, the S1-S3 and the S1-S4 soil systems.

For example, while the frequencies of the dominant shear modes of the sites are calculated as 1.67 Hz, 1.37 Hz and 1.10 Hz in the S1-S2, the S1-S3 and the S1-S4 soil systems, the same values for the frequencies of the coupled sway modes of the soil-pipe interaction systems are obtained as 1.21 Hz, 0.88 Hz and 0.64 Hz with a decrease of 27.54%, 35.77% and 41.82%, respectively. As can be understood, for layered soil systems, the differences between the dominant site frequency values considered with the simplified approach and the dominant frequency values obtained from the soil-pipe interaction model have significantly increased from the S1-S1 to the S1-S4. In addition, it is worth emphasizing here again that these modes obtained for the S1-S2, the S1-S3 and the S1-S4 soil systems are the dominant modes (Table 4). In addition, it may be considered as the coupled shear mode for the soil-pipe interaction system, as seen in Figure 2b, Figure 2c and Figure 2d.

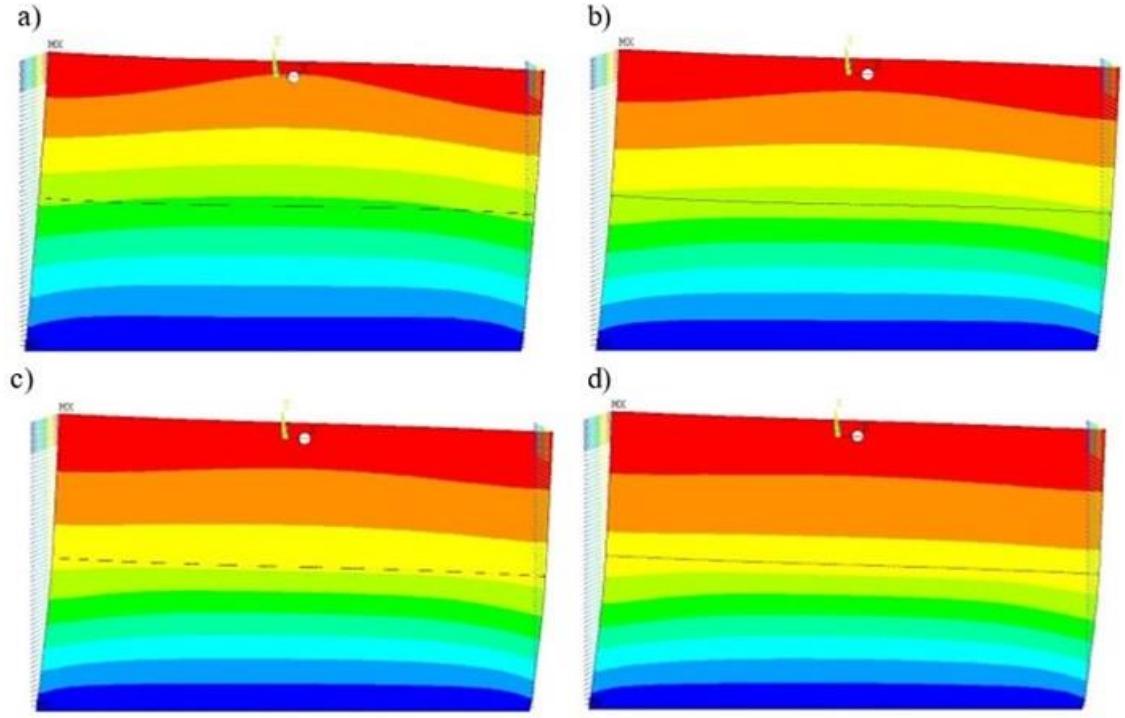

Figure 2. Dominant mode shape of soil-pipe interaction system in a) the S1-S1, b) the S1-S2, c) the S1-S3 and d) the S1-S4 soil system

4.2. Effect of soil-pipe interaction system on responses of pipe system

Depending on the soil-pipe interaction system, the dynamic behavior of the pipe system can change significantly under different soil conditions. Table 5 shows the displacement and von Mises stress responses obtained from the pipe system in four different soil conditions under earthquake loadings. The change in the soil-pipe stiffness ratio can significantly affect the peak dynamic displacements of the pipe system. It is understood that this change in the stiffness ratio causes a decrease in the displacement responses from the S1-S1 to the S1-S4 for all earthquake loadings (Figure 3). For example, while the stiffness ratio is 402.50 in the S1-S4 soil condition, the same ratio is obtained as 715.55 in S1-S1 soil condition. On the other words, while the peak dynamic displacement is 0.222 m in the S1-S4 soil condition

under NF-1 loading, the same response is obtained as 0.348 m with an 56.76% increase depending on decrease of the stiffness ratio in the S1-S4 soil system. A similar trend can be observed under FF-1 loading. For example, under FF-1 loading, the peak dynamic displacement obtained as 0.013 m in S1-S4 soil condition have obtained as 0.045 m with an increase of 246.15% in the S1-S1 soil-condition. Examples of this increasing trend can be increased. For example, under NF-2 loading, the peak dynamic displacement in the S1-S3 soil condition is 0.044 m, while the same response is obtained as 0.090 m increasing by 104.54% in the S1-S1 soil condition.

Table 5. Responses obtained from the pipe system under loadings

Earthquake		Soil profile			
	Response	S1-S1	S1-S2	S1-S3	S1-S4
NF-1	$\lvert U_D \rvert$ (m)	0.348	0.323	0.281	0.222
	V_m (MPa)	230.21	229.12	228.02	225.68
FF-1	$\lvert U_D \rvert$ (m)	0.045	0.035	0.023	0.013
	V_m (MPa)	227.61	227.40	226.25	224.09
NF-2	$\lvert U_D \rvert$ (m)	0.090	0.067	0.044	0.026
	V_m (MPa)	230.48	229.51	227.43	224.61
FF-2	$\lvert U_D \rvert$ (m)	0.033	0.030	0.026	0.018
	V_m (MPa)	227.15	227.08	226.01	223.98
NF-3	$\lvert U_D \rvert$ (m)	0.298	0.236	0.162	0.094
	V_m (MPa)	234.67	232.86	229.73	225.92
FF-3	$\lvert U_D \rvert$ (m)	0.024	0.021	0.018	0.015
	V_m (MPa)	227.04	226.84	225.74	223.80

U_D (m): Absolute peak displacement of pipe system, V_m: Peak von Mises stress of pipe system

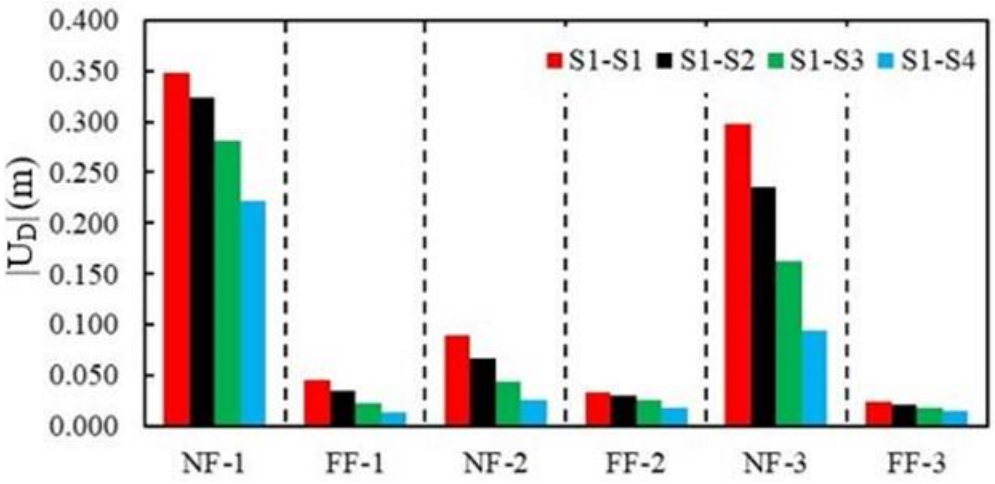

Figure 3. Peak displacements of the pipe system under earthquakes

Comparisons made for displacements can be made within the von Mises stress values. Examining this response is important for understanding the elastic or plastic deformation status in the pipe system depending on the yield stress. When Figure 4 is examined, it is understood that the von Mises stresses of the pipe system under different ground motion loadings increase from the S1-S4 to the S1-S1 depending on decrease in soil stiffness ratio, but it is seen that these changes are relatively limited. For example, the von Mises stress obtained as 224.09 MPa in the S1-S4 soil condition under FF-1 loading is obtained as 227.61 MPa with an increase of 1.57% in the S1-S1 soil condition. NF-3 loading can be used to see example of a similar trend. For example, while the von Mises stress is 225.92 MPa in the S1-S4 soil condition under this loading, the same response shows an increase of 3.87% as 234.67 MPa in the S1-S1 soil condition.

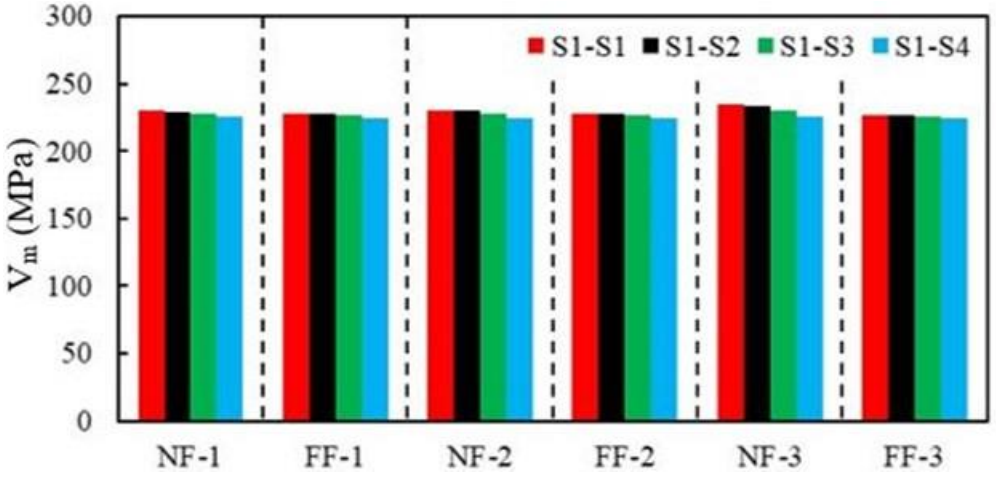

Figure 4. Peak von Mises stresses of the pipe system under earthquakes

4.3. Effects of near-fault and far-fault earthquakes on responses of pipe system

The dynamic behavior of the pipe system can be affected by near-fault and far-fault earthquakes. The degree of this effect can vary depending on the characteristics of the soil-pipe interaction system and earthquakes. In this context, comparisons of peak dynamic displacements obtained using different soil conditions for near-fault and far-fault earthquakes are shown in Figure 5.

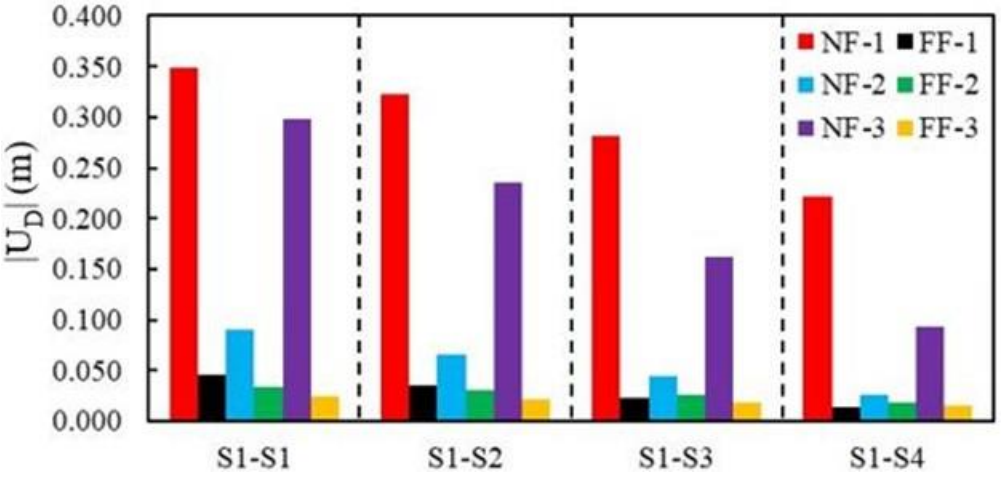

Figure 5. Displacements obtained from the pipe system under earthquakes considered in different soil systems

When Figure 5 is analyzed, it is seen that while the peak dynamic displacement obtained from the pipe system in the S1-S1 soil system under FF-1 loading is 0.045 m, the similar response is calculated as 0.348 m with an increase of 673.33% under NF-1 loading. It is understood that a similar change occurs with an increase of 172.73% under NF-2 loading compared to FF-2 loading in the same soil condition. Similar trends can be seen in other soil systems as well. For example, while the peak dynamic displacement of the pipe under FF-1 loading in the S1-S4 soil condition is 0.013 m, it is seen that the similar response is calculated as 0.222 m increasing by 1607.69% under NF-1 loading. It is understood that this change for the same soil condition occurs with an increase of 526.67% for NF-2 loading compared to the peak dynamic response obtained for FF-3 loading. It is clear from the examples discussed that in all of the soil conditions considered, the near-fault earthquakes cause the greater peak dynamic displacements than those obtained under far-fault earthquakes.

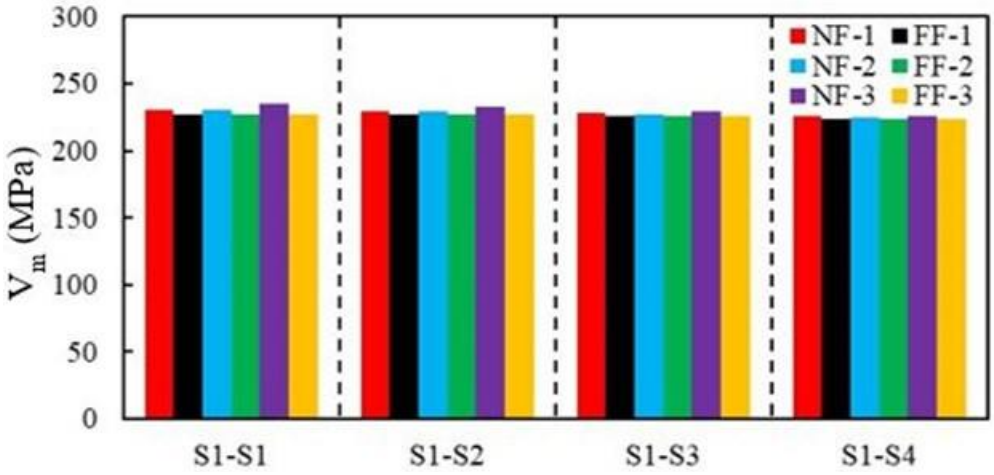

Figure 6. Von Mises stresses obtained from the pipe system under earthquakes considered in different soil systems

It is also possible to observe the response changes obtained under earthquakes using von Mises stresses. For this purpose, when Figure 6 is examined, it is understood that the earthquake loadings considered for different soil systems do not cause a significant change on the von Mises stresses. Although the greater stresses are generally obtained under near-fault loadings compared to far-fault loadings, it is understood that the response changes are relatively limited. For example, when this situation is examined for the peak von Mises stresses obtained in the S1-S1 soil condition, it is understood that the peak response of pipe system under the NF-1 loading is obtained with an increase of 1.14% compared to the FF-1 loading. In addition, this change for the NF-3 realizes as an increase 3.36% compared to the FF-3. Furthermore, when the same response comparisons are made for the S1-S4 soil condition, it is understood that the peak von Mises stress of the pipe system realizes as an increase of 0.71% under the NF-1 loading compared with those of FF-1 loading. This response change for the same conditions under NF-3 loading occurs as a 0.95% increase compared to FF-3 loading.

5. Conclusion

The dynamic behavior of the pipe system can be significantly affected by the characteristics of the soil-pipe interaction system and earthquake loading. In this context, various parametric analyzes have been performed using the finite element model of the soil-pipe interaction system modeled in 2D within the scope of the study. For this purpose, the developed soil-pipe interaction system has been subjected to modal analysis by considering four different soil conditions and before the dynamic loading stage has been started, the dominant mode frequencies of the soil-pipe interaction system have been identified and compared to the dominant site frequencies. In the dynamic loading stage, three near-fault and three far-fault earthquakes from the bedrock level have been applied to the interaction model. The results have been examined by considering the displacement of the pipe system and von Mises stresses, and the obtained findings have been listed below.

- Dominant frequencies of both the site and the soil-pipe interaction system from S1-S1 to S1-S4 soil conditions decrease depending on the decrease in the soil-pipe stiffness.
- The peak dynamic displacements of the pipe system depend significantly on the stiffness ratio between the soil and the pipe systems. Under the model conditions and earthquake loadings considered, the decrease in this ratio results in a decrease in the peak dynamic displacements of the pipe system.
- The pipe system has produced the greater peak dynamic displacement responses under near-fault earthquake loadings compared to far-fault earthquake loadings.
- It is observed that under the boundary conditions and assumptions taken into account, the von Mises stresses of the pipe system are not significantly affected by the soil-pipe interaction system and the near/far-fault earthquakes. These effects have led to a change of less than 5% on the von Mises stresses in the parametric studies conducted within the scope of study.

In this study, two earthquakes with different moment magnitude values have been used. Furthermore, soil-pipe interaction has been investigated under the near-fault and far-fault earthquakes. Findings have been evaluated for soil properties and earthquake characteristics. In this context, in future studies, more earthquakes with different moment magnitude values can be selected and the relationships between moment magnitude and pipe responses can be investigated. In addition, only a single steel pipe with a specific diameter and embedment depth has been used. Therefore, the changes in pipe responses can be examined by taking into account different pipe diameters, materials and embedment depths. Fragility analyses can be carried out by considering different pipe types (steel, PVC, HDPE, etc.), pipe diameters, more near-fault and far-fault earthquakes, soil-pipe stiffnesses. Comparatively examining the different responses of near-fault and far-fault earthquakes on pipelines will contribute to the development of more realistic seismic fragility models. The creation of such models is an important step in reducing seismic risk and increasing design safety in engineering applications.

It is particularly important to emphasize here that the results obtained within the scope of this study are a result of the 2D model, boundary conditions, material and geometric properties taken into account, as well as the earthquake records used. For these reasons, although the results presented within the scope of the study provide a relative perspective to researchers and engineers, generalization of the results to a significant extent is possible by conducting more parametric studies.

Conflict of Interest

The author of the article declares that he has no personal or financial conflict of interest with any institution, organization or person.

References

[1] Unal EO, Kocaman S, Gokceoglu C. Impact assessment of geohazards triggered by 6 February 2023 Kahramanmaras Earthquakes (Mw 7.7 and Mw 7.6) on the natural gas pipelines. Eng Geol 2024;334:107508. https://doi.org/10.1016/j.enggeo.2024.107508.
[2] Vazouras P, Karamanos SA, Dakoulas P. Finite element analysis of buried steel pipelines under strike-slip fault displacements. Soil Dyn Earthq Eng 2010;30:1361–76. https://doi.org/10.1016/j.soildyn.2010.06.011.
[3] Xu L, Cheng X, Huang R, Chen W, Hu W. Local buckling behavior of buried pipeline under seismic oblique-reverse fault displacement. Sci Rep 2022;12:1–17. https://doi.org/10.1038/s41598-022-24728-y.
[4] Saiyar M, Ni P, Take WA, Moore ID. Response of pipelines of differing flexural stiffness to normal faulting. Géotechnique 2016;66:275–86. https://doi.org/10.1680/jgeot.14.P.175.
[5] Wang Y, Xu T, Zhang S, Qin G. Intelligent framework for reliability evolution of natural gas pipelines subjected to earthquakes. Thin-Walled Struct 2025;214:113414. https://doi.org/10.1016/j.tws.2025.113414.
[6] Pan H, Li C, Li H-N, Hu J, Ma R. Underwater shaking table test and seismic fragility assessment of free-spanning submarine pipelines under offshore spatial motions. Thin-Walled Struct 2025;213:113276. https://doi.org/10.1016/j.tws.2025.113276.
[7] Darvishi R, Jafarian Y, Lashgari A. Fragility Analysis of Buried Pipelines Subjected to Seismic Landslides in Iran. J Earthq Eng 2025;00:1–19. https://doi.org/10.1080/13632469.2025.2496653.
[8] Toprak S, Wham BP, Nacaroglu E, Ceylan M, Dal O. Performance of water systems during the February 6th Kahramanmaras earthquakes. Earthq Spectra 2025;41:322–53. https://doi.org/10.1177/87552930241293571.
[9] Uckan E, Aksel M, Atas O, Toprak S, Kaya ES. The performance of transmission pipelines on February 6th, 2023 Kahramanmaras earthquake: a series of case studies. Bull Earthq Eng 2025;23:1203–22. https://doi.org/10.1007/s10518-024-01957-2.
[10] Hindy A, Novak M. Earthquake response of underground pipelines. Earthq Eng Struct Dyn 1979;7:451–76. https://doi.org/10.1002/eqe.4290070506.
[11] Datta TK, Mashaly EA. Pipeline response to random ground motion by discrete model. Earthq Eng Struct Dyn 1986;14:559–72. https://doi.org/10.1002/eqe.4290140406.
[12] Takada S, Hassani N, Fukuda K. A new proposal for simplified design of buried steel pipes crossing active faults. Earthq Eng Struct Dyn 2001;30:1243–57. https://doi.org/10.1002/eqe.62.

[13] Pan H, Li H-N, Li C. Seismic fragility analysis of free-spanning submarine pipelines incorporating soil spatial variability in soil-pipe interaction and offshore motion propagation. Eng Struct 2023;280:115639. https://doi.org/10.1016/j.engstruct.2023.115639.
[14] Pan H, Li H-N, Li C. Seismic behaviors of free-spanning submarine pipelines subjected to multi-support earthquake motions within offshore sites. Ocean Eng 2021;237:109606. https://doi.org/10.1016/j.oceaneng.2021.109606.
[15] Datta TK. Seismic analysis of structures. Chichester, UK: John Wiley & Sons, Ltd; 2010. https://doi.org/10.1002/9780470824634.
[16] Anastasopoulos I, Gerolymos N, Drosos V, Kourkoulis R, Georgarakos T, Gazetas G. Nonlinear response of deep immersed tunnel to strong seismic shaking. J Geotech Geoenvironmental Eng 2007;133:1067–90. https://doi.org/10.1061/(ASCE)1090-0241(2007)133:9(1067).
[17] ANSYS Inc. ANSYS Mechanical APDL [Computer Software] 2015.
[18] Sun W, Lin J, Ma Q, Yan S, Tong H, Liang Q. Seismic fragility assessment of circular metro tunnels in loess deposit. J Cent South Univ 2024;31:950–64. https://doi.org/10.1007/s11771-024-5592-9.
[19] Akl SA, Metwally KG. Optimizing arching creation for Abou Muharik Tunnel in Egypt using numerical analysis. KSCE J Civ Eng 2017;21:160–7. https://doi.org/10.1007/s12205-016-0428-2.
[20] Düzgün OA, Hatipoğlu YS. Effective Damping Coefficient of Fluid Viscous Dampers for Dynamic Response Mitigation of Coupled Frames. J Vib Eng Technol 2023;11:1821–35. https://doi.org/10.1007/s42417-022-00673-y.
[21] Lysmer J, Kuhlemeyer RL. Finite dynamic model for infinite media. J Eng Mech Div 1969;95:859–77. https://doi.org/10.1061/JMCEA3.0001144.
[22] Kramer SL, Stewart JP. Geotechnical Earthquake Engineering. vol. 1. Boca Raton: CRC Press; 2024. https://doi.org/10.1201/9781003512011.
[23] Abate G, Fiamingo A, Massimino MR. An eco-sustainable innovative geotechnical technology for the structures seismic isolation, investigated by FEM parametric analyses. Bull Earthq Eng 2023;21:4851–75. https://doi.org/10.1007/s10518-023-01719-6.
[24] Ozturk KF, Cakir T, Araz O. A comparative study to determine seismic response of the box culvert wing wall under influence of soil-structure interaction considering different ground motions. Soil Dyn Earthq Eng 2022;162:107452. https://doi.org/10.1016/j.soildyn.2022.107452.
[25] Zangeneh A, François S, Lombaert G, Pacoste C. Modal analysis of coupled soil-structure systems. Soil Dyn Earthq Eng 2021;144:106645. https://doi.org/10.1016/j.soildyn.2021.106645.
[26] Livaoğlu R, Doğangün A. Simplified seismic analysis procedures for elevated tanks considering fluid–structure–soil interaction. J Fluids Struct 2006;22:421–39. https://doi.org/10.1016/j.jfluidstructs.2005.12.004.
[27] Cakir T. Evaluation of the effect of earthquake frequency content on seismic behavior of cantilever retaining wall including soil–structure interaction. Soil Dyn Earthq Eng 2013;45:96–111. https://doi.org/10.1016/j.soildyn.2012.11.008.
[28] Bardet JP. Experimental soil mechanics. New Jersey: Prentice Hall; 1997.
[29] Bekdaş G, Kayabekir AE, Nigdeli SM, Toklu YC. Tranfer function amplitude minimization for structures with tuned mass dampers considering soil-structure interaction. Soil Dyn Earthq Eng 2019;116:552–62. https://doi.org/10.1016/j.soildyn.2018.10.035.
[30] Fema P695. Quantification of building seismic performance factors. Fema P695 2009:421.
[31] Soyluk K, Karaca H. Near-fault and far-fault ground motion effects on cable-supported bridges. Procedia Eng 2017;199:3077–82. https://doi.org/10.1016/j.proeng.2017.09.421.
[32] Li S, Xie L. Progress and trend on near-field problems in civil engineering. Acta Seismol Sin 2007;20:105–14. https://doi.org/10.1007/s11589-007-0105-0.
[33] Sun B, Zhang S, Deng M, Wang C. Inelastic dynamic response and fragility analysis of arched hydraulic tunnels under as-recorded far-fault and near-fault ground motions. Soil Dyn Earthq Eng 2020;132:106070. https://doi.org/10.1016/j.soildyn.2020.106070.
[34] Zhang C, Zhao M, Zhong Z, Du X. Seismic Intensity Measures and Fragility Analysis for Subway Stations Subjected to Near-fault Ground Motions with Velocity Pulses. J Earthq Eng 2022;26:8724–50. https://doi.org/10.1080/13632469.2021.1994056.
[35] Cao V Van, Ronagh HR. Correlation between seismic parameters of far-fault motions and damage indices of low-rise reinforced concrete frames. Soil Dyn Earthq Eng 2014;66:102–12. https://doi.org/10.1016/j.soildyn.2014.06.020.
[36] Mei X, Sheng Q, Cui Z. Effect of Near-Fault Pulsed Ground Motions on Seismic Response and Seismic Performance to Tunnel Structures. Shock Vib 2021;2021:1–18. https://doi.org/10.1155/2021/9999007.

[37] Zhang S, Wang G. Effects of near-fault and far-fault ground motions on nonlinear dynamic response and seismic damage of concrete gravity dams. Soil Dyn Earthq Eng 2013;53:217–29. https://doi.org/10.1016/j.soildyn.2013.07.014.
[38] Pacific Earthquake Engineering Research (PEER) Center. PEER ground motion database 2021. https://ngawest2.berkeley.edu/.
[39] Ozturk KF. Investigation of the effects of mainshock-aftershock sequences on the dynamic responses of pipeline considering soil-pipeline interaction. Tunn Undergr Space Technol 2025;155:106231. https://doi.org/10.1016/j.tust.2024.106231.
[40] Yoshida N. Seismic Ground Response Analysis. vol. 36. Dordrecht: Springer Netherlands; 2015. https://doi.org/10.1007/978-94-017-9460-2.